

NEUTRAL-CURRENT QUARK COUPLING DETERMINATION
USING NEUTRINO-NEUTRON AND NEUTRINO-PROTON
DEEP-INELASTIC CROSS SECTIONS*

L. F. Abbott and R. Michael Barnett
Stanford Linear Accelerator Center
Stanford University, Stanford, California 94305

ABSTRACT

There is some question about the reliability of inclusive-pion-production analyses as used in previous determinations of the weak neutral-current couplings of u and d quarks. We are able to eliminate this input altogether by using new neutrino and antineutrino data for the ratio of neutral-current neutron-to-proton deep-inelastic cross sections, $\sigma(\nu n \rightarrow \nu X) / \sigma(\nu p \rightarrow \nu X)$. Another new input to our model independent analysis is the Q^2 dependence of elastic neutrino-proton scattering. The final values determined for the neutral-current couplings are consistent with those we obtained previously. For purposes of comparison, we also present a new analysis of high-energy inclusive-pion data.

(Submitted to Phys. Rev. D.)

*Research supported in part by the Department of Energy under contract number EY-76-C-03-0515.

The weak neutral-current couplings of u and d quarks have recently been determined by analyses of deep-inelastic and elastic neutrino-scattering and neutrino-induced inclusive and exclusive-pion-production processes.^{1,2} However, a weak point in past determinations has been their dependence on low-energy inclusive-pion-production ($\nu N \rightarrow \nu \pi X$) data.³ In evaluating these data, extensive parton-model assumptions are made which might be suspect, especially at such low energies.

This situation can be improved by using new results on inclusive-pion production at high energies. We present an analysis of these data⁴ below. A possible problem with these data is that one must subtract out kaons and protons from the experimental numbers to obtain the desired pion multiplicities. In addition, analyses of inclusive-pion data require extensive use of final-state quark fragmentation ideas. Fortunately, we find that all of the difficulties associated with inclusive-pion data and their analysis can be completely avoided by using new results on the ratio of neutral-current neutron-to-proton deep-inelastic cross sections ($R \equiv \sigma(\nu n \rightarrow \nu X)/\sigma(\nu p \rightarrow \nu X)$). These give us the same isospin information about the neutral current as the inclusive-pion data and can be evaluated using only the conventional parton-model assumptions of deep-inelastic scattering. Thus, the neutral-current couplings of u and d quarks can now be determined without using any quark fragmentation models.

The quark coupling constants to be determined are the parameters u_L , d_L , u_R and d_R in the effective neutrino-quark interaction Lagrangian

$$\mathcal{L} = \frac{G}{\sqrt{2}} \bar{\nu} \gamma^\mu (1 + \gamma_5) \nu \left[u_L \bar{u} \gamma_\mu (1 + \gamma_5) u + u_R \bar{u} \gamma_\mu (1 - \gamma_5) u + d_L \bar{d} \gamma_\mu (1 + \gamma_5) d + d_R \bar{d} \gamma_\mu (1 - \gamma_5) d \right] . \quad (1)$$

We will restrict ourselves to values of the quark couplings which are allowed by our previous analysis¹ of deep-inelastic neutrino scattering ($\nu N \rightarrow \nu X$) off an isoscalar target. In our present analysis, the determination then begins by considering the ratio of neutron-to-proton deep-inelastic cross sections.⁵ The resulting allowed values are then further restricted by an analysis^{1,2} of the magnitude and Q^2 dependence of elastic neutrino-proton scattering cross sections. (In our previous work (Ref. 1) only the total elastic cross sections were considered.) Additional restrictions on the allowed couplings are imposed by exclusive-pion-production ($\nu N \rightarrow \nu N\pi$) data⁷ evaluated as in Ref. 1. The quark coupling values resulting from the present analysis are:^{8,9}

$$\begin{aligned} u_L &= .29 \pm .14 & u_R &= -.16 \pm .07 \\ d_L &= -.41 \pm .11 & d_R &= 0 \pm .16 \end{aligned} \quad (2)$$

where errors show 90% confidence limits and an overall sign convention ($u_L \geq 0$) has been assumed. These values are entirely consistent with those determined in Ref. 1 where the analysis included low-energy inclusive-pion data. The errors shown here are significantly larger than those of Ref. 1; however, no inclusive-pion data are used.

The neutral-current neutron-to-proton deep-inelastic cross section ratios, $\sigma(\nu n \rightarrow \nu X)/\sigma(\nu p \rightarrow \nu X)$, for neutrinos and for antineutrinos written in terms of the quark coupling constants u_L , d_L , u_R and d_R assuming an SU(2) symmetric sea are:

$$R_{n/p}^{\nu} = \frac{u_L^2 + 2d_L^2 + \xi(u_R^2 + 2d_R^2) + \alpha'(u_R^2 + d_R^2 - d_L^2 + \xi(u_L^2 + d_L^2 - d_R^2))}{d_L^2 + 2u_L^2 + \xi(d_R^2 + 2u_R^2) + \alpha'(d_R^2 + u_R^2 - u_L^2 + \xi(d_L^2 + u_L^2 - u_R^2))} \quad (3)$$

$$R_{n/p}^{\bar{\nu}} = \frac{u_R^2 + 2d_R^2 + \bar{\xi}(u_L^2 + 2d_L^2) + \alpha'(u_L^2 + d_L^2 - d_R^2 + \bar{\xi}(u_R^2 + d_R^2 - d_L^2))}{d_R^2 + 2u_R^2 + \bar{\xi}(d_L^2 + 2u_L^2) + \alpha'(d_L^2 + u_L^2 - u_R^2 + \bar{\xi}(d_R^2 + u_R^2 - u_L^2))} \quad (4)$$

where

$$\xi = \frac{\int dE_{\nu} E_{\nu} \rho_{\nu} \int_{E_0/E_{\nu}}^1 dy (1-y)^2}{\int dE_{\nu} E_{\nu} \rho_{\nu} \int_{E_0/E_{\nu}}^1 dy} \quad (5)$$

$$\bar{\xi} = \frac{\int dE_{\bar{\nu}} E_{\bar{\nu}} \rho_{\bar{\nu}} \int_{E_0/E_{\bar{\nu}}}^1 dy (1-y)^2}{\int dE_{\bar{\nu}} E_{\bar{\nu}} \rho_{\bar{\nu}} \int_{E_0/E_{\bar{\nu}}}^1 dy} \quad (6)$$

and

$$\alpha' = \frac{3\alpha}{2+\alpha} \quad (7)$$

with E_0 the hadronic energy cutoff ($E_{\text{hadron}} > E_0$), ρ_{ν} and $\rho_{\bar{\nu}}$ the spectra of incoming neutrinos and antineutrinos and α the ratio of antiquarks to quarks. The experimental values of these ratios with $\xi = .21$, $\bar{\xi} = .13$ and $\alpha' = .12$ are⁵

$$R_{n/p}^{\nu} = 1.22 \pm 0.35 \quad (8)$$

and

$$R_{n/p}^{\bar{\nu}} = .53 \pm .39 \quad (9)$$

Using these data in conjunction with results from deep-inelastic scattering off an isoscalar target¹⁰ gives the allowed coupling constants shown in Fig. 1. The annuli in Fig. 1 indicate values of the quark couplings allowed by the isoscalar deep-inelastic scattering data. The four regions shaded with dots show the values allowed by the above

neutron-to-proton cross section ratios at the 90% confidence level.

In order to show correlations between left and right coupling constants it is convenient to use the parametrization:

$$\begin{aligned} u_L &= r_L \sin \theta_L & u_R &= r_R \sin \theta_R \\ d_L &= r_L \cos \theta_L & d_R &= r_R \cos \theta_R \end{aligned} \tag{10}$$

As Fig. 1 indicates, the allowed values of r_L and r_R are quite well determined by the isoscalar deep-inelastic scattering data. However, these data give no information about the allowed values of θ_L and θ_R . Such information comes from the neutron-to-proton deep-inelastic scattering data considered above. The values of θ_L and θ_R allowed at the 90% confidence level by these ratios are shown by the regions shaded with dots in Figs. 2-4. In all three of these figures we have fixed the left radial value ($r_L = .53$) at the center of the allowed annulus of Fig. 1(a) since variations within the allowed annulus produce little effect. In Fig. 2 we have taken the right radial value ($r_R = .22$) at the outer edge of the allowed annulus of Fig. 1(b); in Fig. 3 we choose a radial value ($r_R = .175$) at the center of this allowed annulus, and in Fig. 4 we take a radius ($r_R = .13$) at the inner edge. All of the figures show four allowed regions (shaded with dots) which are in good qualitative agreement with the four regions allowed by low-energy inclusive-pion-production data (see Ref. 1). However, the allowed regions of Figs. 1-4 are considerably larger than those coming from the low-energy inclusive-pion results.

The four regions allowed by this new analysis of neutron-to-proton deep-inelastic cross section ratios can be further restricted by using

elastic and exclusive-pion-production data as in Ref. 1. We first consider the elastic data by comparing the magnitude and Q^2 dependence of elastic neutrino-proton scattering cross sections with those for various values of the quark couplings and requiring agreement at the 90% confidence level (using a χ^2 test of fit). We have included the 20% systematic uncertainty along with the statistical errors in these data and view this as essential for a reliable analysis. The resulting allowed values of θ_L and θ_R are shown in Figs. 2-4 by the areas shaded with lines and contained by dotted curves. The consequences of the Q^2 analysis are very similar to the results of our analysis of the total elastic cross sections in Ref. 1.

We now include the restrictions imposed by exclusive-pion-production data evaluated as in Ref. 1. The values of θ_L and θ_R allowed by both the elastic and exclusive-pion analyses are the cross-hatched areas of Figs. 2-4. Note that portions of region D (the upper left-hand dotted region) are allowed by elastic data, but are completely eliminated by exclusive-pion results. Furthermore, virtually all of the overlap between the elastic and the neutron-to-proton ratio results in region B (the lower right-hand dotted region) is eliminated by the exclusive-pion data.

The final values of θ_L and θ_R which are consistent with all data are shown in Figs. 2-4 by both cross-hatching and shading with dots. The allowed values are almost exclusively in region A (the upper right-hand dotted region). Very small allowed areas also occur inside region B (the lower right-hand dotted region) for the radial values $r_R = .175$ and $r_R = .13$, but are at the edge of the 90% confidence limits. These have been ignored in the quark coupling values of Eq. (1).

The final allowed values for u_L , d_L , u_R and d_R are plotted in Fig. 1 where they are shown shaded with lines. In Fig. 1, we have also plotted the quark coupling values of the Weinberg-Salam model¹¹ for $\sin^2 \theta_W = 0.0, 0.1, \dots, 0.7$. Clearly, our results are in excellent agreement with this model for $\sin^2 \theta_W$ in the range $0.2 \leq \sin^2 \theta_W \leq 0.3$.

It is interesting to go back and compare the results from our analysis of the ratios of neutron-to-proton deep-inelastic cross sections with new data⁴ on high-energy inclusive-pion production ($\nu N \rightarrow \nu \pi X$) by both neutrinos and antineutrinos. We have used SLAC electroproduction results¹² to subtract out kaons, protons and antiprotons from the total charged particle multiplicities reported for neutrino data in order to get pion multiplicities. We have assumed that electroproduction ratios of K/π , p/π and \bar{p}/π in the same general kinematic range are applicable to the neutrino data. The analysis then proceeds as in Ref. 1. At the 90% confidence level, the allowed values of u_L , d_L , u_R and d_R are shown in Fig. 5 shaded with dots and likewise the allowed values of θ_L and θ_R for the radial values $r_L = .53$ and $r_R = .175$ are shown in Fig. 6. Note that the allowed four regions are in excellent agreement with the analogous four regions coming from the neutron-to-proton cross section ratios as shown shaded with dots in Figs. 1 and 3. The agreement is particularly striking because it comes from two completely different types of analyses.

We conclude with a table of the experimental values^{4-7,10,13,14} we have used here and in Ref. 1 to determine the neutral-current couplings¹⁵ compared with the predictions of the Weinberg-Salam model for $\sin^2 \theta_W = .25$.

Acknowledgments

We would like to acknowledge useful conversations with C. Baltay, J. Bjorken, S. Brodsky, G. Feldman, F. Gilman, J. Marriner, J. Martin, F. Nezeck, B. Roe, J. Strait, L. Sulak and H. Williams. Both authors would like to thank the Aspen Center for Physics and one of us (R.M.B.) would like to thank Brookhaven National Laboratory for the stimulating atmosphere those institutions provided and for their hospitality. This research was supported in part by the Department of Energy under contract number EY-76-C-03-0515.

REFERENCES

1. L. F. Abbott and R. M. Barnett, Phys. Rev. Lett. 40, 1303 (1978) and Phys. Rev. D 18, 3214 (1978).
2. J. J. Sakurai, Phys. Rev. Lett. 35, 1037 (1976); P. Q. Hung and J. J. Sakurai, Phys. Lett. 63B, 295 (1976), 69B, 323 (1977) and 72B, 208 (1977); S. Weinberg, Phys. Rev. D 5, 1412 (1972); M. Barnett, Phys. Rev. D 14, 2990 (1976); C. H. Albright *et al.*, Phys. Rev. D 14, 1780 (1976); V. Barger and D. V. Nanopoulos, Nucl. Phys. B124, 426 (1977); J. J. Sakurai and L. F. Urrutia, Phys. Rev. D 11, 159 (1975); D. P. Sidhu, Phys. Rev. D 14, 2235 (1976); F. Martin, Nucl. Phys. B104, 111 (1976); P. Scharbach, Nucl. Phys. B82, 155 (1974); P. Q. Hung, Phys. Lett. 69B, 216 (1977); L. M. Sehgal, Phys. Lett. 71B, 99 (1977); S. L. Adler, Ann. Phys. 40, 189 (1968) and Phys. Rev. D 12, 2644 (1975); S. L. Adler *et al.*, Phys. Rev. D 12, 3501 (1975) and D 13, 1216 (1976); E. H. Monsay, Argonne report ANL-HEP-PR-78-08 (1978) and Phys. Rev. Lett. 41, 728 (1978); G. Ecker, Phys. Lett. 72B, 450 (1978); D. P. Sidhu and P. Langacker, Phys. Rev. Lett. 41, 732 (1978) and Phys. Lett. 74B, 233 (1978); E. A. Paschos, Brookhaven report no. BNL-24619 (1978) and Phys. Rev. D 15, 1966 (1977); R. E. Hendrick and L.-F. Li, Carnegie-Mellon report (June 1978); S. Sarkar, Pennsylvania report (July 1978); two recent papers have analyzed the Q^2 dependence of elastic vp scattering directly: M. Claudson, E. A. Paschos and L. R. Sulak, report submitted to the XIX International Conference on High Energy Physics, Tokyo, 23-30 August 1978; H. H. Williams, report presented at the XIX International Conference on High Energy Physics, Tokyo, 23-30 August 1978.

3. H. Kluttig et al., Phys. Lett. 71B, 446 (1977).
4. J. Marriner (neutrinos), report no. LBL-6438 (1977), University of California Ph.D. thesis; B. Roe (antineutrinos), Michigan report, invited talk at the Topical Conference on Neutrino Physics at Accelerators, Oxford, England, July 4-9, 1978.
5. J. Marriner (neutrinos), report no. LBL-6438 (1977), University of California Ph.D. thesis; W. C. Louis (antineutrinos), University of Michigan Ph.D. thesis (1978).
6. L. R. Sulak, Harvard report, to appear in the Proc. of the Neutrinos-78 Conference, Lafayette, Indiana, April 28-May 2, 1978; H. H. Williams, Pennsylvania report, presented at the Oxford Neutrino Conference, Oxford, England, July 4-7, 1978; J. B. Strait and W. Kozanecki, Harvard University Ph.D. thesis (1978); see also: W. Lee et al., Phys. Rev. Lett. 37, 186 (1976); M. Pohl et al., Phys. Lett. 72B, 489 (1978); see also M. Claudsen et al., and H. H. Williams in Ref. 2.
7. W. Krenz et al., Nucl. Phys. B135, 45 (1978); O. Erriques et al., Phys. Lett. 73B, 350 (1978); see also: S. J. Barish et al., Phys. Rev. Lett. 33, 448 (1974); W. Lee et al., Phys. Rev. Lett. 38, 202 (1977).
8. If the limits on u_L , d_L , u_R and d_R found from our analysis of the new high-energy inclusive-pion-production data⁴ are included in the final determination of quark couplings, then we obtain:

$$\begin{array}{ll} u_L = 0.35 \pm 0.08 & u_R = -0.16 \pm 0.07 \\ d_L = -0.38 \pm 0.09 & d_R = 0 \pm 0.16 \end{array}$$

9. The values expected in the Weinberg-Salam model¹¹ for $\sin^2 \theta_W = 0.25$ are:
- | | |
|---------------|---------------|
| $u_L = 0.33$ | $u_R = -0.17$ |
| $d_L = -0.42$ | $d_R = 0.08$ |
10. M. Holder et al., Phys. Lett. 72B, 254 (1977); see also:
J. Blietschau et al., Nucl. Phys. B118, 218 (1977); A. Benvenuti et al., Phys. Rev. Lett. 37, 1039 (1976); P. Wanderer et al., Phys. Rev. D 17, 1679 (1978); F. S. Merritt et al., Phys. Rev. D 17, 2199 (1978); P. C. Bosetti et al., Phys. Lett. 76B, 505 (1978).
11. S. Weinberg, Phys. Rev. Lett. 19, 1264 (1967); A. Salam, in Elementary Particle Physics: Relativistic Groups and Analyticity (Nobel Symposium No. 8), edited by N. Svartholm (Almqvist and Wiksell, Stockholm, 1968), p. 367.
12. J. F. Martin et al., report no. SLAC-PUB-2161 (1978).
13. F. J. Hasert et al., Phys. Lett. 46B, 121 (1973); J. Blietschau et al., Nucl. Phys. B114, 189 (1976); H. Faissner et al., Phys. Rev. Lett. 41, 213 (1978); A. M. Cnops et al., Phys. Rev. Lett. 41, 357 (1978); F. Reines et al., Phys. Rev. Lett. 37, 315 (1976); P. Alibrand et al., Phys. Lett. 74B, 422 (1978); M. Haguenaer, invited talk at the XIX International Conference on High Energy Physics, Tokyo, 23-30 August 1978; the weighted averages for $\nu_\mu e$ and $\bar{\nu}_\mu e$ were taken from: C. Baltay, invited talk at the XIX International Conference on High Energy Physics, Tokyo, 23-30 August 1978.
14. C. Y. Prescott et al., report no. SLAC-PUB-2148 (1978).
15. An interesting question (brought to our attention by S. Glashow, T. D. Lee and W. Marciano) concerns the extent to which purely

left-handed neutral currents can be ruled out. Taking $u_R = d_R = 0$ (but not assuming any particular V-A model), the CDHS deep-inelastic total cross sections¹⁰ require $u_L^2 + d_L^2 = 0.306 \pm 0.025$, and we find from other types of data that best fits are obtained if $\theta_L \approx 135^\circ$ so that $u_L \approx -d_L \approx 0.39 \pm 0.02$ (at 90% confidence). As can be seen in Fig. 1(b), CDHS data alone exclude $u_R = d_R = 0$; however, this follows primarily from the y-dependence of their neutral-current data.¹⁰ Those authors state that the exclusion of pure V-A is at the 4 standard deviation level (which could conceivably be affected by the new analysis which CDHS has applied to their charged-current data). It is useful, nonetheless, to see if this result can be confirmed by other types of data. Both the high-energy inclusive-pion data⁴ and the neutron-to-proton deep-inelastic data⁵ are entirely consistent with $u_R = d_R = 0$. In contrast, elastic νp data⁶ exclude V-A by 2.5 standard deviations if $u_L = -d_L = 0.37$ and by more if $u_L = -d_L > 0.37$. Furthermore, the exclusive-pion data⁷ (at the 90% confidence level) require $u_L = -d_L > 0.37$. Turning to the question of the electron's neutral-current couplings (e_L and e_R), the $\nu_\mu e$ and $\bar{\nu}_\mu e$ data¹³ and the SLAC polarized-electron asymmetry¹⁴ are entirely consistent with $e_R = 0$ and $e_L = 0.37-0.39$. However, the data¹³ for $\bar{\nu}_e e$ are about 3 standard deviations from consistency with $e_R = 0$ (for all e_L allowed by $\nu_\mu e$ and $\bar{\nu}_\mu e$ data). In conclusion we believe that the data which provide the strongest and most verifiable restrictions on $u_R = d_R = 0$ are those from deep-inelastic scattering, so that additional such results would be useful. Nonetheless, it appears now that V-A is in some contradiction with three types of experiments.

TABLE CAPTION

- I. A compendium of neutral-current data compared with values predicted by the Weinberg-Salam model for $\sin^2 \theta_W = 0.25$. Data are from Refs. 4-7, 10, 13, 14. All errors shown indicate 90% confidence limits and a 30% theoretical uncertainty has been indicated for exclusive-pion-production processes.

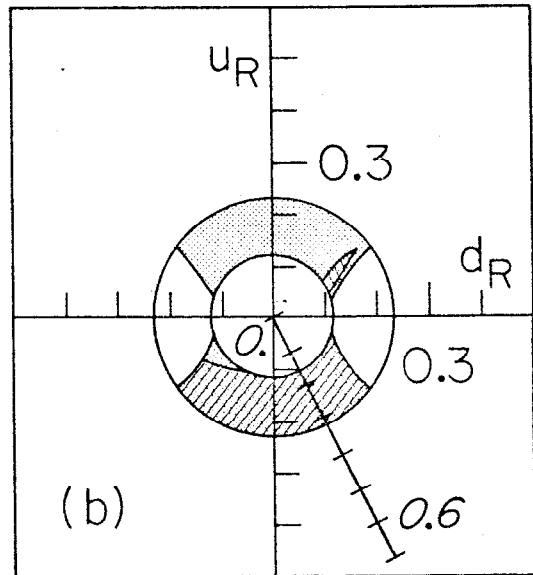
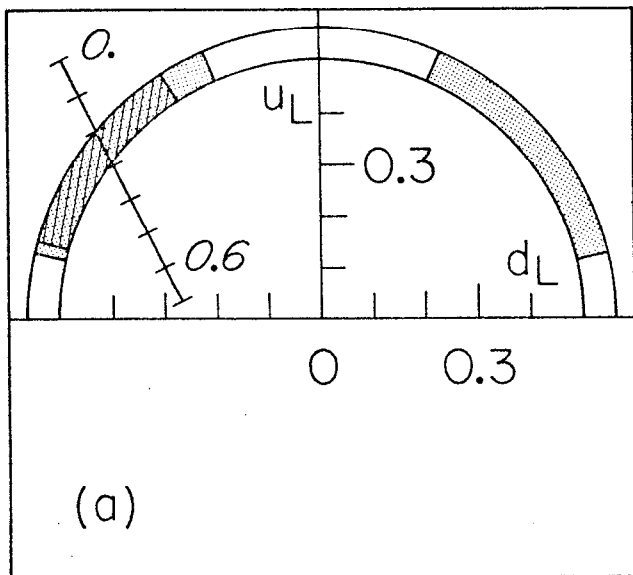
Table I

Process	Quantity Measured	Data with 90% Confidence Experimental limits (Statistical + Systematics)	WS Theory $\sin^2 \theta_W = 0.25$
$\nu N \rightarrow \nu X$	R	$.295 \pm .02$.31
$\bar{\nu} N \rightarrow \bar{\nu} X$	R	$.34 \pm .05$.36
$(\nu n \rightarrow \nu X) / (\nu p \rightarrow \nu X)$	R	$1.22 \pm .56$	1.13
$(\bar{\nu} n \rightarrow \bar{\nu} X) / (\bar{\nu} p \rightarrow \bar{\nu} X)$	R	$.53 \pm .62$.92
$\nu N \rightarrow \nu \pi X$	N_{π^+} / N_{π^-}	$.86 \pm .32$.86
$\bar{\nu} N \rightarrow \bar{\nu} \pi X$	N_{π^+} / N_{π^-}	$1.27 \pm .91$	1.19
$\nu p \rightarrow \nu p$	R	$.11 \pm .05$.11
$\bar{\nu} p \rightarrow \bar{\nu} p$	R	$.19 \pm .10$.12
$\nu p \rightarrow \nu p \pi^0$	R	$.56 \pm .16$	$.42 \pm .13$
$\nu n \rightarrow \nu n \pi^0$	R	$.34 \pm .15$	$.43 \pm .13$
$\nu n \rightarrow \nu p \pi^-$	R	$.45 \pm .20$	$.28 \pm .08$
$\nu p \rightarrow \nu n \pi^+$	R	$.34 \pm .12$	$.28 \pm .08$
$\bar{\nu} N \rightarrow \bar{\nu} N \pi^0$	R	$.57 \pm .16$	$.39 \pm .12$
$\bar{\nu} n \rightarrow \bar{\nu} p \pi^-$	R	$.58 \pm .26$	$.29 \pm .09$
$\nu_{\mu} e \rightarrow \nu_{\mu} e$	$\frac{\sigma}{E} \left(\frac{\text{cm}^2}{\text{GeV}} \right)$	$(1.7 \pm 0.8) \times 10^{-42}$	1.4×10^{-42}
$\bar{\nu}_{\mu} e \rightarrow \bar{\nu}_{\mu} e$	$\frac{\sigma}{E} \left(\frac{\text{cm}^2}{\text{GeV}} \right)$	$(1.8 \pm 1.5) \times 10^{-42}$	1.4×10^{-42}
$\bar{\nu}_e e \rightarrow \bar{\nu}_e e (1.5 < E_e < 3.0)$	$\sigma \text{ (cm}^2\text{)}$	$(5.96 \pm 2.7) \times 10^{-43}$	5.94×10^{-43}
$\bar{\nu}_e e \rightarrow \bar{\nu}_e e (3.0 < E_e < 4.5)$	$\sigma \text{ (cm}^2\text{)}$	$(3.21 \pm 1.3) \times 10^{-43}$	2.53×10^{-43}
$e_{\text{pol}} N \rightarrow e X$	$A/Q^2 \left(\frac{1}{\text{GeV}^2} \right)$	$(9.5 \pm 2.6) \times 10^{-5}$	7.2×10^{-5}

FIGURE CAPTIONS

1. The left (a) and right (b) coupling-constant planes. The lower half of (a) is omitted due to our sign convention $u_L \geq 0$. The annular regions are allowed by deep-inelastic data off an isoscalar target. The regions shaded with dots are allowed by results on the ratios of neutron-to-proton deep-inelastic cross sections, and the regions shaded with lines are allowed by elastic and exclusive-pion data as well. The lines with tick-marks indicate quark coupling values of the Weinberg-Salam model for $\sin^2 \theta_W = 0.0, 0.1, \dots, 0.7$.
2. The allowed angles in the coupling planes of Fig. 1 for fixed radii taken at the center of the allowed annulus ($r_L = 0.53$) in the left-coupling plane and at the outer edge of the allowed annulus ($r_R = 0.22$) in the right-coupling plane. The elliptical regions shaded with dots show areas allowed by the neutron-to-proton deep-inelastic cross section ratios; going clockwise from the upper right, they are regions A, B, C and D respectively. The area shaded with lines and enclosed by a dotted curve is allowed by the magnitude and Q^2 -dependence of elastic data. The region which is cross-hatched is allowed by both elastic and exclusive-pion-production data. The final allowed region is both cross-hatched and shaded with dots.
3. Same as Fig. 2 except that the radius in the right-coupling plane ($r_R = 0.175$) has been chosen at the center of the allowed annulus from Fig. 1(b).
4. Same as Fig. 2 except that the radius in the right-coupling plane ($r_R = 0.13$) has been chosen at the inner edge of the allowed annulus from Fig. 1(b).

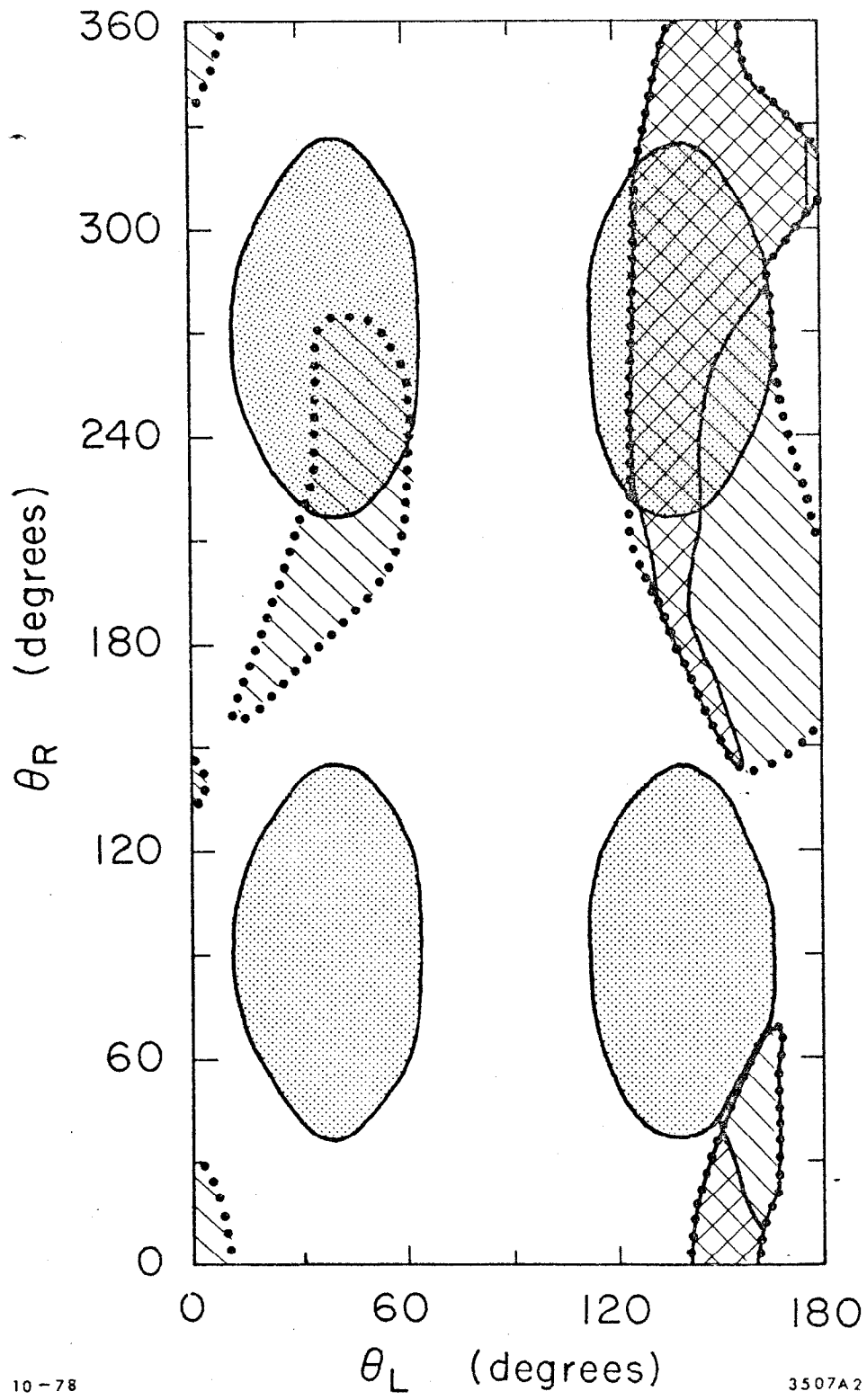
5. The left (a) and right (b) coupling-constant planes. The annular regions are allowed by isoscalar deep-inelastic data as in Fig. 1. The regions shaded with dots are allowed by high-energy inclusive-pion-production data.
6. The regions shaded with dots show angles in the coupling planes of Fig. 5 which are allowed by high-energy inclusive-pion data, for radii taken at the centers of the allowed annulii ($r_L = 0.53$ and $r_R = 0.175$).



10-78

3507A1

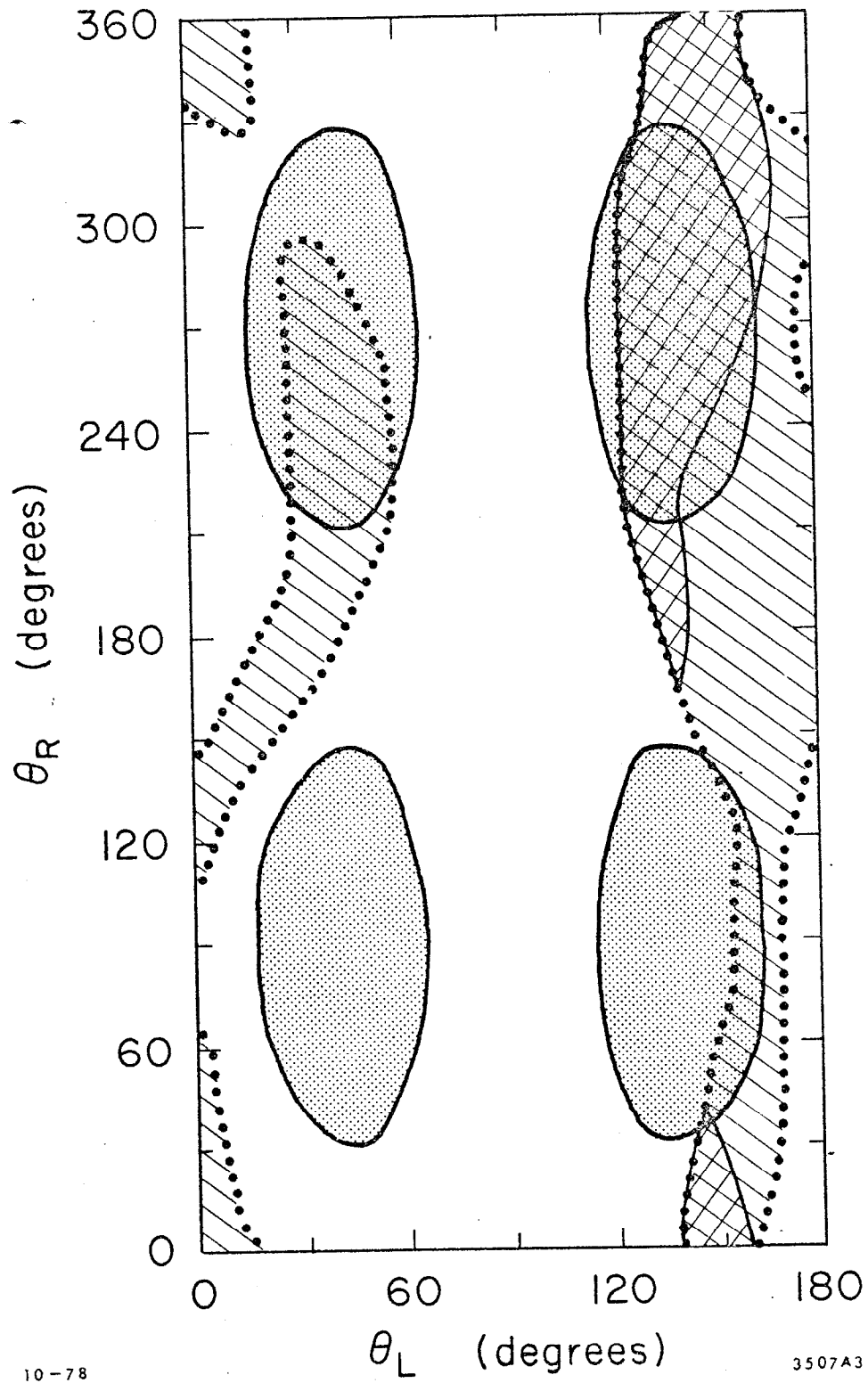
Fig. 1



10-78

3507A2

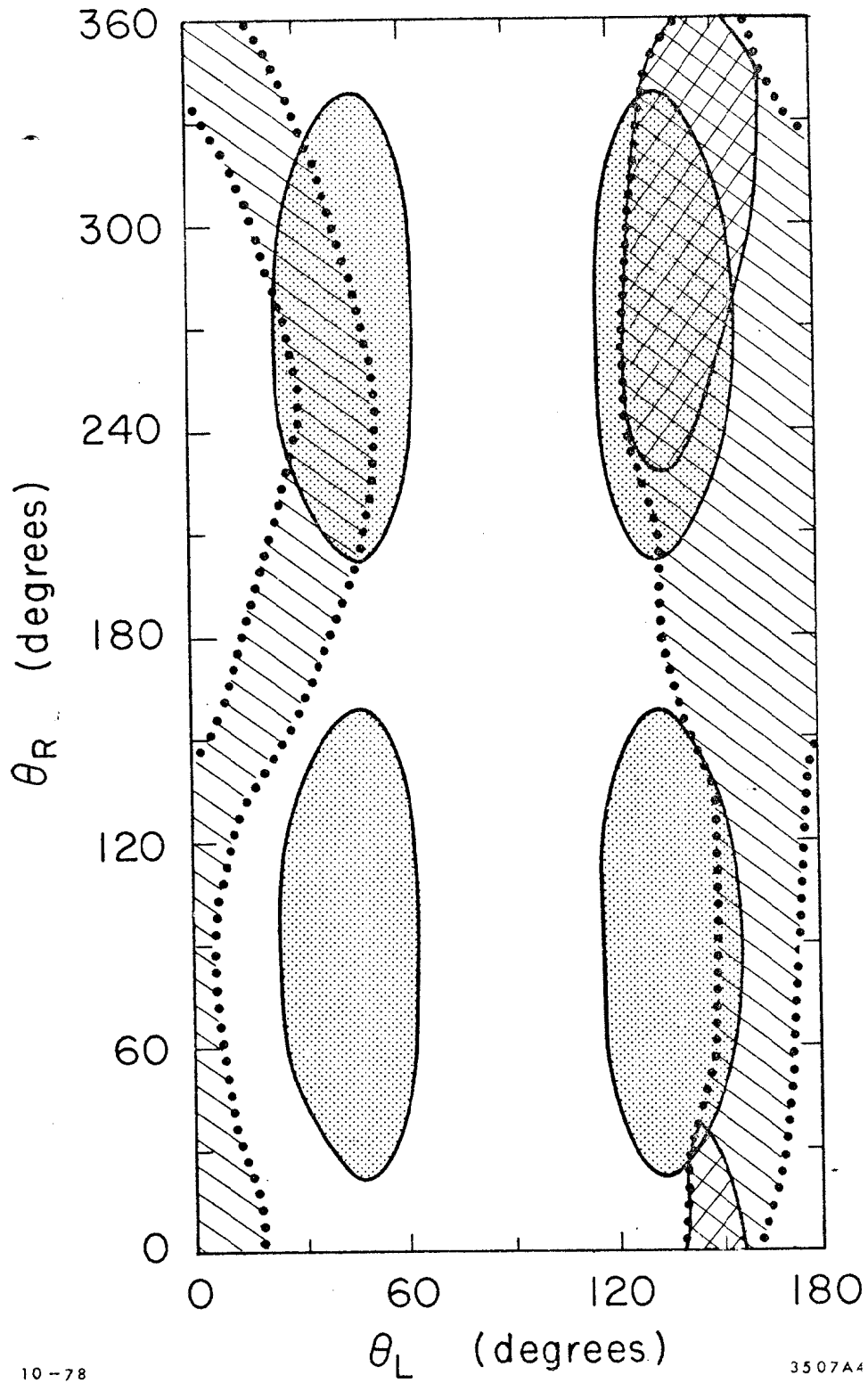
Fig. 2



10-78

3507A3

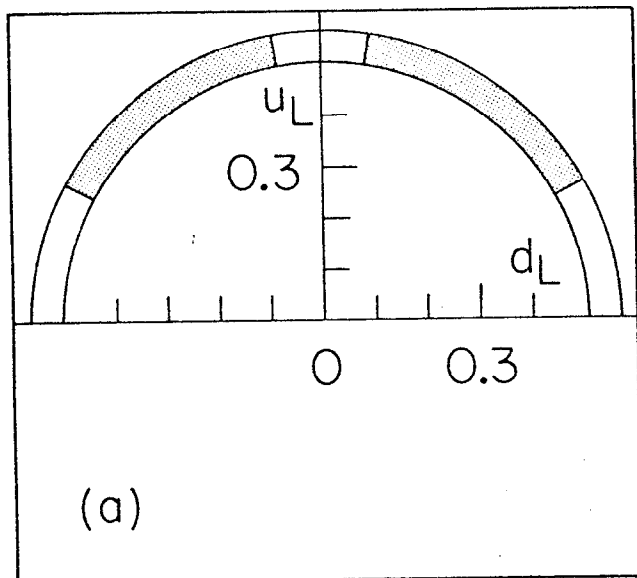
Fig. 3



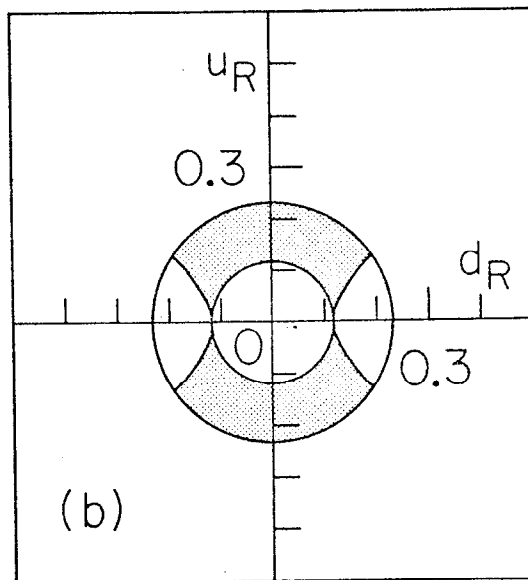
10-78

3507A4

Fig. 4

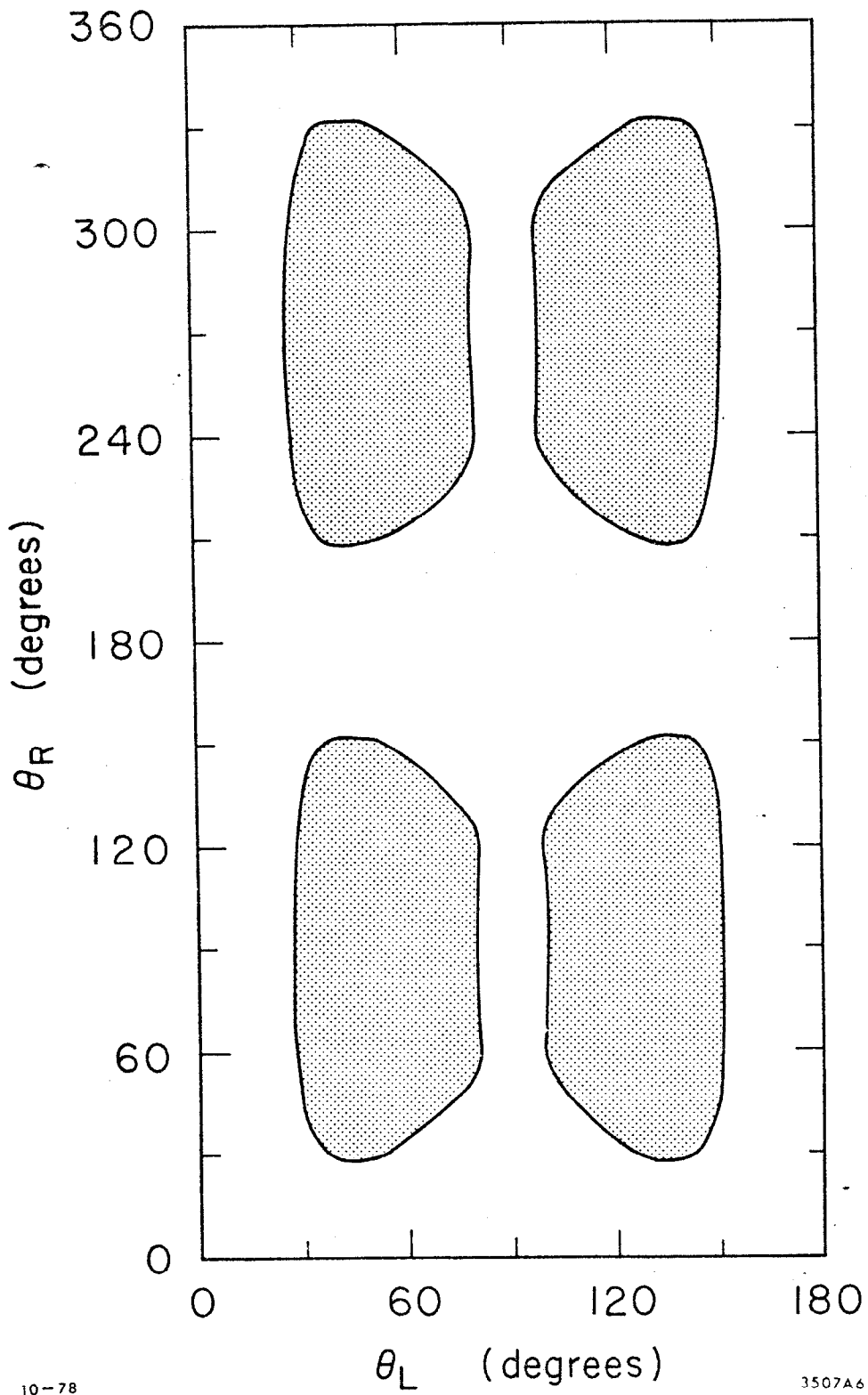


10-78



3507A5

Fig. 5



10-78

3507A6

Fig. 6